Dynamic stability and manipulation of bright matter-wave solitons by optical lattices in Bose–Einstein condensates*

Song Chang-Sheng(宋昌盛), Li Jing(黎 菁), and Zong Feng-De(宗丰德)†

Institute of Nonlinear Physics, Zhejiang Normal University, Jinhua 321004, *China*

(Received 9 June 2011; revised manuscript received 10 August 2011)

An extended variation approach to describing the dynamic evolution of self-attractive Bose–Einstein condensates is developed. We consider bright matter-wave solitons in the presence of a parabolic magnetic potential and a time-space periodic optical lattice. The dynamics of condensates is shown to be well approximated by four coupled nonlinear differential equations. A noteworthy feature is that the extended variation approach gives a critical strength ratio to support multiple stable lattice sites for the condensate. We further examine the existence of the solitons and their stabilities at the multiple stable lattice sites. In this case, the analytical predictions of Bose–Einstein condensates variational dynamics are found to be in good agreement with numerical simulations. We then find a stable region for successful manipulating matter-wave solitons without collapse, which are dragged from an initial stationary to a prescribed position by a moving periodic optical lattice.

Keywords: Bose–Einstein condensates, Gross–Pitaevskii equation, matter-wave solitons, controlled manipulation

PACS: 03.75.Lm, 05.45.Yv, 42.65.Tg **DOI:** 10.1088/1674-1056/21/2/020306

1. Introduction

In recent years a large number of research groups across the world have generated Bose–Einstein condensates (BECs) by bringing various dilute gases to extremely low temperatures via laser and evaporative cooling methods.[1] Interactions between atoms forming BECs result in a rich variety of physical phenomena,[2−9] ranging from matter-wave (MW) optics to accurate measurements and quantum information processing. The progress in experimental and theoretical studies of BECs has led to an increase of interesting in MW solitons. Much of the MW soliton research has been aimed at exploiting, manipulating, and characterizing macroscopic quantum phenomena,[2] including phase coherence,[3] MW diffraction,[4] quantum logic,[5] MW transport,[6] MW gratings, and pulsed MW lasers.[7]

The study of the MW solitons has become a fundamentally interesting topic. Solitons may be trapped, transferred, and manipulated similarly to what has been recently demonstrated experimentally and theoretically. Feshbach technology for generating attractive or repulsive BECs[10] is becoming, relatively speaking, commonplace. In general, an effective setting for the creation of matter-wave solitons in BECs is provided by parabolic traps, as well as in usual optical lattice (OL),[11] which are induced, through interference patterns, by coherent laser beams illuminating the condensates in opposite directions. Additionally, the lattice shape and its depth can be readily tuned by varying the propagation angles and the intensities of the lattice-creating light beams.[12] The possibility to control the OL has led to the realization of many interesting phenomena, including Landau–Zener tunneling,[13] Bloch oscillations,[14] and quantum superfluid-insulator transitions.[15] Indeed, external electromagnetic fields can also be used to trap and manipulate BECs.[16] Furthermore, the manipulation of coherent nonlinear MW structures[17] in trapped BECs has indeed received some examinations. Notice that MW solitons may travel a long distance in a real experiment, up to several millimeters,[18] and are truly robust objects, being themselves coherent condensate.

*Project supported by the National Natural Science Foundation of China (Grant Nos. 10672147 and 11072219), the Natural Science Foundation of Zhejiang Province, China (Grant Nos. Y605312 and Y1080959), and the Foundation of Department of Education of Zhejiang Province, China (Grant No. 20030704).

†Corresponding author. E-mail: fdzong@zjnu.cn

© 2012 Chinese Physical Society and IOP Publishing Ltd

As such, the ability to control and manipulate the condensate has now become a central issue for the physics of BECs.

The objective of this work is to systematically study the dynamics and manipulation of one-dimensional (1D) bright MW solitons in the combination of the parabolic magnetic trap and OL potentials. Specifically, we apply an extended variational approach (EVA) to the governing nonlinear partial differential equation, which reduces the BEC dynamics to a much simpler set of four coupled nonlinear differential equations, which capture the amplitude, chirp, central position, and central-frequency fluctuations observed in simulations and experiment. More especially, multiple stable lattice sites are obtained by the variational method. With respect to the external potential, the trapping and the manipulation of the condensate in numerous lattice sites are fundamentally interesting. Our analysis characterizes the dynamics from one lattice site to another and predicts when the multiple lattice sites are stable. More importantly, the analysis also suggests how to selectively control the condensate by means of a moving OL. Additionally, it is the first time that we have examined the possibility of finding a stable region for successful controlled dragging of solitons from a fixed point of one stable site to a prescribed position via modulating a time-dependent OL in the presence of a parabolic potential. It means that a condensate loaded with information will transmit undistortedly over a long time in the system. In particular, it is very important to guide the manipulation of bright solitons in experiment, and it may provide a useful and an effective method of storing and processing quantum information.

The rest of the present paper is organized as follows. In Section 2, the governing mean-field equation is presented. In Section 3, we analyse the stability subjected to the EVA dynamic system. In Section 4, the manipulation properties of the MW solitons are numerically investigated and then a stable region for successful dragging of the condensate is found. The results of the work are summarized in Section 5.

2. Governing equation

The Gross–Pitaevskii equation (GPE),[19] which governs the evolution of the wave function in the mean-field approximation, takes its fundamental form in the three-dimensional (3D) case. A number of studies analyse its reduction to an effective 1D equation in the case of strongly elongated cigar-shaped BECs.[20] A general conclusion is that the effective equation reduces to the straightforward 1D version of the GPE in the normalized form

$$\mathrm{i}u_t = -\frac{1}{2}u_{xx} + g|u|^2u + V(x)u, \tag{1}$$

where $u(x,t)$ is the 1D mean-field wave function. The BECs are assumed to be confined by the following potential in which the combination of an OL and a parabolic trap is considered:

$$V(x) = V_0\cos\left[2k(x-\bar{x})\right] + V_1x^2. \tag{2}$$

In Eqs. (1) and (2), x is measured in units of the fluid healing length $\xi = \hbar/\sqrt{n_0gm}$, where n_0 is the peak density and $g = 4\pi\hbar^2\alpha m^{-1}\int|\phi(y,z)|^4\mathrm{d}y\mathrm{d}z = 2\alpha\hbar\omega_\perp$ is the effective 1D interaction strength (α is the scattering length, m the atomic mass, and $w_\perp$ the corresponding oscillator frequency). Additionally, $V_1 = 1/2\Omega^2 \ll 1$, where $\Omega \equiv \hbar\omega_x/gn_0$ (ω_x is the confining frequency in the axial direction) determines the parabolic trap strength.[18] Therefore, the range of V_1 is about 10^{-5}–10^{-2}. While $V_0 = sE_\mathrm{R}$ is the OL strength, where $E_\mathrm{R} = \hbar^2k^2/2m$ is the recoil energy, s the dimensionless strength, and k the wave number of the OL. The strength of OL can be readily tuned by varying the intensities of the lattice-creating light beams, and the wave number of OL can be controlled by varying the angle θ between the counterpropagation laser beams which produce the interference pattern with the wavelength $\lambda \equiv 2\pi/k = (\lambda_\mathrm{laser}/2)\sin(\theta/2)$,[21] where λ_laser is the wavelength of the laser beams producing the OL. The parameter $\bar{x}$ measures the offset of a minimum of the OL with respect to the minimum of the parabolic potential. More specifically, it provides a possibility to manipulate the condensate in our work. In this case, g ($g = \pm1$) is the renormalized nonlinear coefficient, which is positive (negative) for a repulsive (attractive) condensate. As we are interested in the ordinary bright MW solitons, which exist in the case of attraction, we will fix $g = -1$.

To estimate actual physical quantities corresponding to the above normalized values of the parameters, we must restrict our study of BECs to a safe range, in which the system becomes effectively 1D; i.e., the energy of interatomic interactions is much less than the kinetic energy in the transverse direction:[22]

$\varepsilon^2 = \alpha_\perp/\xi^2 \sim N|\alpha|/\alpha_0 \ll 1$. The bright soliton in BECs has been created with the parameters of $N \simeq 10^3, w_\perp = 2\pi \times 710$ Hz, and $w_x = 2\pi \times 50$ Hz for ^{7}Li.[23] Then, for a 1D peak density $n_0 = 10^8$ m^{-1}, the time and the space units correspond to 0.3 ms and 1.64 μm, respectively. To sum up, these offer a range of available theoretical parameters for our work in this paper.

In the case where $V(x) = 0$, the governing equation (1) reduces to the nonlinear Schrödinger equation for which soliton solutions are known to exist.[24] More specifically, the stability and the dynamics of the one-soliton solution plays a critical role in determining the behaviour in BEC systems. Two standard methods have been developed to characterize the behaviour of the one-soliton under perturbation: soliton perturbation theory[25] and the variational method.[26] Unfortunately, standard soliton perturbation theory is incapable of reproducing the dynamics observed in the numerical simulations considered here since it fails to capture the quadratic phase changes, which drive the amplitude-width fluctuations. However, the EVA generally provides a quantitative characterization of the dynamics.

3. Variational dynamics and analysis of stability

In many issues of nonlinear optics and BECs,[27,28] variational methods are proposed. In general, the variational methods have been used extensively for Hamiltonian systems. To apply the EVA to the present model, we notice that equation (1) can be derived from the Lagrangian density[24] given by

$$\mathscr{L} = \mathrm{i}\left(u\frac{\partial u^*}{\partial t} - u^*\frac{\partial u}{\partial t}\right) + \left|\frac{\partial u}{\partial x}\right|^2 - |u|^4 + 2V(x)|u|^2, \tag{3}$$

where the asterisk denotes the complex conjugation. In order to obtain the dynamics of the condensate in the trapping potential, a Gaussian ansatz is adopted

$$u = A\sqrt{\eta}\exp(-\eta^2(x-x_0)^2 + \mathrm{i}[\beta(x-x_0)^2 + \xi(x-x_0) + \phi]), \tag{4}$$

where variables η, β, x_0, ξ, and ϕ (amplitude, chirp, central position, central frequency, and absolute phase, respectively) each are a real function of time t. Notice that the scaling constant A determines the total number of condensed atoms in the trap to be $N = \int_{-\infty}^{+\infty}|u|^2\mathrm{d}x = \frac{1}{2}A^2\sqrt{2\pi}$. It is possible to calculate the average Lagrangian[29,30] $L = \int_{-\infty}^{+\infty}\mathscr{L}\mathrm{d}x$ using ansatz (4) with Eq. (3). Adopting the Euler Lagrange formulas $\partial L/\partial p = 0$, where p is one of the parameters η, β, x_0, and ξ, gives the reduced dynamical system as

$$\frac{\mathrm{d}\eta}{\mathrm{d}t} = -2\eta\beta, \tag{5}$$

$$\frac{\mathrm{d}\beta}{\mathrm{d}t} = 2(\eta^4 - \beta^2) - \frac{A^2\sqrt{2}}{2}\eta^3 + 2V_0k^2\cos[2k(\bar{x} - x_0)] - V_1, \tag{6}$$

$$\frac{\mathrm{d}x_0}{\mathrm{d}t} = \xi, \tag{7}$$

$$\frac{\mathrm{d}\xi}{\mathrm{d}t} = -2V_1x_0 - 2V_0k\sin[2k(\bar{x} - x_0)]. \tag{8}$$

The four coupled nonlinear differential equations (5)–(8) mentioned above have been simplified by assuming that $k/\eta \ll 1$, thus $\exp[-k^2/2\eta^2] \approx 1$. This assumption holds in the case due to the fact that the localized solution is narrower than the period of the potential. It should be noticed that this simplification allows us to extend recent results[31,32] since stability can be computed explicitly. The nonlinear system of differential equations governs the interactions between the amplitude, chirp, central position, and central frequency. Moreover, it is worth noting that chirp is the only dynamical quantity that couples with amplitude as seen in Eq. (5), thus considering the amplitude fluctuation to be similar to that between central position and central frequency in Eq. (7). This should be different from the soliton perturbation theory, which does not allow for chirp dynamics and therefore disallows amplitude fluctuations for any real potentials $V(x)$. Further, note that the absolute phase variable $\phi(t)$ has nothing to do with dynamics (5)–(8) due to the phase invariance of Eq. (1).

The standard treatment of nonlinear differential equations involves locating their static solutions and determining their linear stability properties,[33] in which the nonlinear coupled equations have been successfully solved on the issue of stability. The steady-state solutions (fixed points) of Eqs. (5)–(8) are found by setting the terms on the right-hand sides to be equal to zero, and the fixed points satisfy the following system:

$$\beta_0 = 0, \tag{9}$$

$$2\eta_0^4 - \frac{A^2\eta_0^3}{\sqrt{2}} + 2V_0k^2\cos[2k(\bar{x} - x_{00})] - V_1 = 0, \tag{10}$$

$$\xi_0 = 0, \tag{11}$$

$$-2V_1x_{00} - 2V_0k\sin[2k(\bar{x} - x_{00})] = 0, \tag{12}$$

where the solutions to these equations are denoted by η_0, β_0, x_{00}, and ξ_0. The linear stability of the fixed points $(\eta, \beta, x_0, \xi) = (\eta_0, 0, x_{00}, 0)$ is established by considering the evolution of the perturbed quantities denoted by triangles:[34] $\eta = \eta_0 + \triangle\eta$, $\beta = 0 + \triangle\beta$, $x_0 = x_{00} + \Delta x_0$, and $\xi = 0 + \Delta\xi$. Substituting these into the general dynamics of the system (5)–(8) results in the following linearized evolution system:

$$\begin{pmatrix} \dfrac{\mathrm{d}\Delta\eta}{\mathrm{d}t} \\ \dfrac{\mathrm{d}\Delta\beta}{\mathrm{d}t} \\ \dfrac{\mathrm{d}\Delta x_0}{\mathrm{d}t} \\ \dfrac{\mathrm{d}\Delta\xi}{\mathrm{d}t} \end{pmatrix} = \begin{pmatrix} 0 & -2\eta_0 & 0 & 0 \\ 8\eta_0^3 - \dfrac{3A^2\eta_0^2}{\sqrt{2}} & 0 & 4V_0k^3\sin[2k(\bar{x}-x_{00})] & 0 \\ 0 & 0 & 0 & 1 \\ 0 & 0 & -2V_1 + 4V_0k^2\cos[2k(\bar{x}-x_{00})] & 0 \end{pmatrix} \begin{pmatrix} \Delta\eta \\ \Delta\beta \\ \Delta x_0 \\ \Delta\xi \end{pmatrix}. \tag{13}$$

Corresponding to the specific dynamical system considered here, the linear system about the steady-state solution gives the matrix as

$$M = \begin{pmatrix} 0 & -2\eta_0 & 0 & 0 \\ 8\eta_0^3 - \dfrac{3A^2\eta_0^2}{\sqrt{2}} & 0 & 4V_0k^3\sin[2k(\bar{x}-x_{00})] & 0 \\ 0 & 0 & 0 & 1 \\ 0 & 0 & -2V_1 + 4V_0k^2\cos[2k(\bar{x}-x_{00})] & 0 \end{pmatrix}. \tag{14}$$

The eigenvalues λ_j $(j = 1, 2, 3, 4)$ of this matrix can be easily calculated and are given by

$$\lambda_{1,2} = \pm\mathrm{i}\sqrt{16\eta_0^4 - 3\sqrt{2}A^2\eta_0^3}, \tag{15}$$

$$\lambda_{3,4} = \pm\mathrm{i}\sqrt{2V_1 - 4V_0k^2\cos[2k(\bar{x}-x_{00})]}. \tag{16}$$

Eigenvalues (15) and (16) determine the stability in the variational dynamics system. It is necessary to notice that the stability can then be established by using eigenvalues (15) and (16). We rewrite the expressions with Eqs. (9)–(12) as

$$\lambda_{1,2} = \pm\mathrm{i}\sqrt{\sqrt{2}A^2\eta_0^3 + 16V_1\left\{\frac{1}{2} - \frac{V_0k^2}{V_1}\cos[2k(\bar{x}-x_{00})]\right\}}, \tag{17}$$

$$\lambda_{3,4} = \pm\mathrm{i}\sqrt{2V_1\left\{1 - 2\frac{V_0k^2}{V_1}\cos[2k(\bar{x}-x_{00})]\right\}}. \tag{18}$$

Notice that the parameter V_0k^2/V_1 has played a key role in determining the stability of the static solutions for the eigenvalues equations. In particular, for $|V_0|k^2/V_1 < 1/2$ (V_0 is a negative value), the eigenvalues are always purely imaginary since the quantities under the square root are strictly positive. On this condition, the governing equation has only one stable solution. In particular, for $|V_0|k^2/V_1 > 1/2$, the values $\lambda_{3,4}$ can alternate between purely imaginary (stable solution) and purely real (unstable saddle) as $\cos[2k(\bar{x}-x_0)]$ oscillates between positive and negative values.

It is obvious that the strength ratio plays a key role in generating multiple stable lattice sites. Thus, only a finite number of fixed points are possible for a given strength of the interaction between the parabolic and OL potentials. The quantity $|V_0|k^2/V_1$ in a suitable range determines the number of the lattice sites. Figure 1 shows three different external complex potentials, which contain five lattice sites as $V_0 = -30$, -50, and -70, while at the same V_1. Here, if we adopt $V_0 < -70$ or $V_0 > -30$, the number of multiple stable lattice sites will change. The number of the lattice sites will increase as the strength ratio $|V_0|k^2/V_1$ is added. Furthermore, the strength of OL is much larger than that of parabolic potential ($V_0 \gg V_1$), which provides the necessary condition for a finite number of stable lattice sites. The following exact

analysis will be elaborated with five stable sites as the parameter $V_0 = -50.0$.

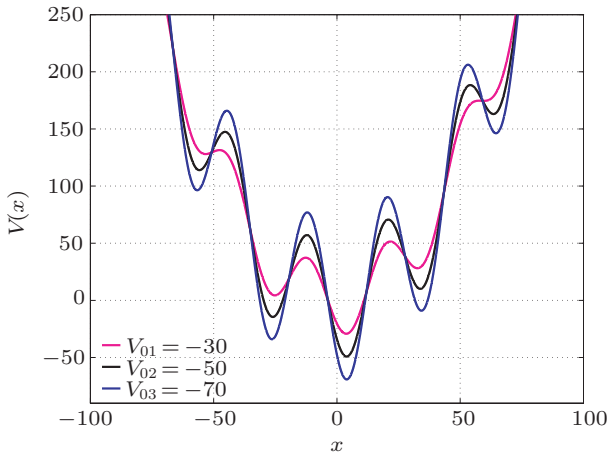


Fig. 1. (colour online) Graphical representation of the five lattice sites with three different values of V_0 in the presence of parabolic magnetic and OL potentials as obtained from Eq. (2). The parameter values are $A = 1.5$, $\bar{x} = 1.25\pi$, $k = 0.1$, and $V_1 = 0.05$.

Table 1. The values of five stable lattice sites (in Fig. 1) corresponding to fixed points (from left to right). The parameter values are $A = 1.5$, $\bar{x} = 1.25\pi$, $k = 0.1$, $V_0 = -50.0$, and $V_1 = 0.05$.

Stable lattice sites ($V(x)$)	115.00	–14.03	–49.27	9.45	161.84
The fixed points (x)	–55.94	–26.17	3.74	33.63	63.32

The following issue that we study is the comparison of predictions of the EVA with numerical results in the dynamics of MW solitons and their stabilities (here, we have chosen five stable lattice sites (fixed points) as seen in Fig. 1, while at $V_{02} = -50$). To check the predictions for the stability and the evolution of the MW soliton and examine the validity of the EVA, we perform the direct simulation with the model Eq. (1) by dint of the higher-order split-step Fourier method (with $n = 2048$, the space step and the time step of the numerical integration are $\Delta x = 0.04$, $\Delta t = 0.001$), which can monitor the basic conserved quantities and the energy of solitons.[35] In the meantime, those sets of nonlinear differential equations (5)–(8) cannot be solved analytically and we resort to their numerical solutions using fourth-order Runge–Rutta method.[34]

Figures 2 and 3 exemplify the typical dynamics, which can result in the system when the five stable fixed points are present in Table 1. The dynamics of Eqs. (5)–(8) at one fixed point ($x_0 = 3.74$) as an original location is shown in Fig. 2. Likewise, Fig. 3 demonstrates the dynamics of the condensate trapped nearby the neighbouring fixed point ($x_0 = 37.15$). In Fig. 3, it is noticeable that the amplitude and the chirp each exhibit a beating-type phenomenon, which results from the fact that the frequency of amplitude-chirp is closer to the frequency of central position in the system. The oscillation of the condensate is more fierce than that in Fig. 2 since the fixed point is no longer at the minimum of the external potential. To sum up, we can draw a conclusion that the whole evolution of WM solitons placed at (nearby) the fixed point demonstrates the existence and their stabilities at the multiple lattice sites in the presence of the parabolic and OL potentials. It is noticeable that the predictions of the EVA are fully consistent with the direct numerical simulation results.

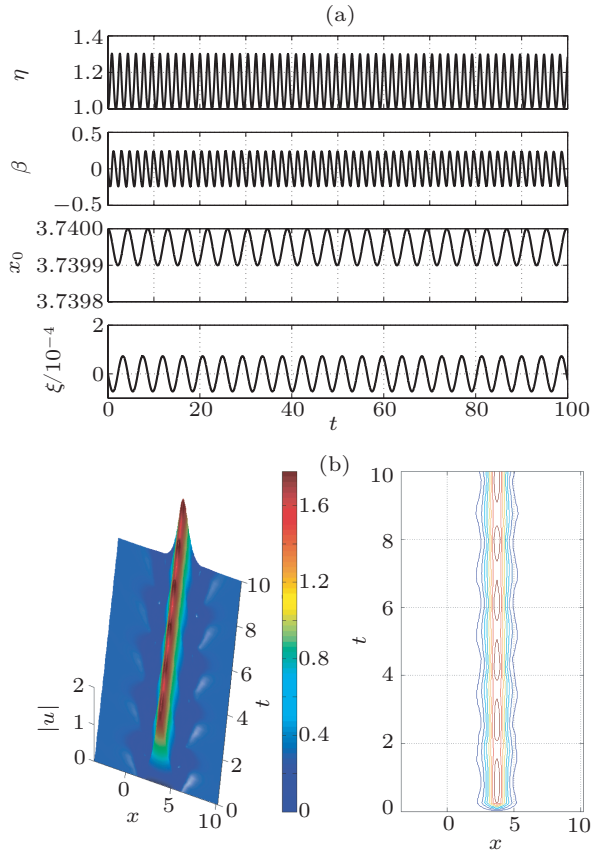


Fig. 2. (colour online) Bright MW solitons dynamics whose initial position is placed in the fixed point at $x_0 = 3.74$. (a) Normalized amplitude (η), chirp (β), central position (x_0), and central frequency (ξ) fluctuation each as a function of time for EVA Eqs. (5)–(8). (b) The evolution plot of $|u|$ by direct numerical simulation and its contour plot based on Eq. (1). The parameter values are $A = 1.5$, $V_0 = -50.0$, $k = 0.1$, $\bar{x} = 1.25\pi$, and $V_1 = 0.05$. The initial conditions are $(\eta,\ \beta,\ x_0,\ \xi) = (1, 0, 3.74, 0)$.

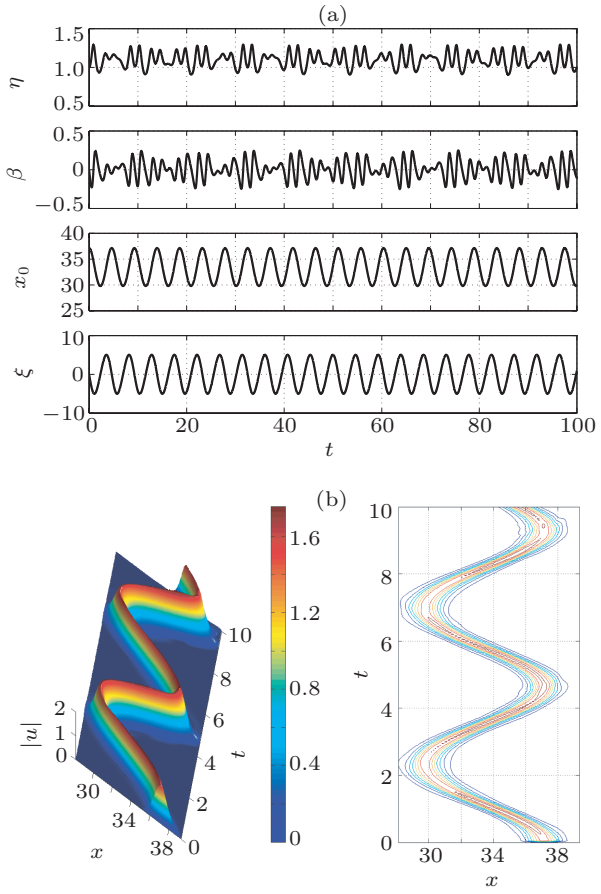


Fig. 3. (colour online) Bright MW solitons dynamics whose initial position is placed nearby the neighbouring fixed point at $x_0 = 37.15$. (a) Normalized amplitude (η), chirp (β), central position (x_0), and central frequency (ξ) fluctuation each as a function of time for EVA Eqs. (5)–(8). (b) The evolution plot of $|u|$ by direct numerical simulation and its contour plot based on Eq.(1). The parameter values are $A = 1.5$, $V_0 = -50.0$, $k = 0.1$, $\bar{x} = 1.25\pi$, and $V_1 = 0.05$. The initial conditions are $(\eta,\ \beta,\ x_0,\ \xi) = (1, 0, 37.15, 0)$.

4. Manipulation of MW solitons

Having addressed the existence and the stability of the MW solitons, we then concentrate our attention upon the manipulation of the condensate. The solitons are set to be in motion by offsetting the OL and are observed to propagate in the potential for many oscillatory cycles without collapse.[36] Here, we proceed to the consideration of a mentioned possibility and the manipulation of a stationary bright MW soliton (initially trapped at a fixed point of the external potential) by a steadily moving OL. More specifically, the OL may be used as a means of moving the soliton in a prescribed way, i.e., as a "robotic arm" depositing the soliton at a desired location. Note that similar results have also been obtained (see Ref. [37]), but here we aim to consider a more complicated problem, namely finding a stable region to manipulate the MW solitons via modulating the moving OL in the presence of a parabolic magnetic trap. Additionally, it is necessary to point out the selection of our theoretical parameters of the manipulation dynamics in BECs is refered to the experimental results (see Refs. [18] and [23]).

In this case, we rewrite the complex potential Eq. (2) in the following form:

$$V(x) = V_0 \cos\left[2k(x - y(t))\right] + V_1 x^2, \tag{19}$$

where the position of the OL is translated according to[38]

$$y(t) = x_{\rm i} + \frac{1}{2}(x_{\rm f} - x_{\rm i})\left[1 + \tanh\left(\frac{t - t^*}{\tau}\right)\right], \tag{20}$$

where the initial and the final positions of the condensate are $x_{\rm i}$ and $x_{\rm f}$, respectively. Additionally, τ and t^* are controlled manipulation constants. The adiabaticity parameter τ controls the acceleration of the centre $y(t)$. The instant of maximum acceleration is

$$t^* = \tanh^{-1}\sqrt{(1 - \epsilon\tau)}\tau, \tag{21}$$

where ϵ is a small parameter, ϵ=0.001, such that the initial velocity of the soliton is negligible. Likewise, $y(0) \approx x_{\rm i}$ and $y(2t^*) \approx x_{\rm f}$ hold true faultlessly. This condition on t^* allows for the reduction of parameters and allows us to ensure that we begin with an initial position very close to the centre of the fixed point ($y(0) \approx 0$) and that we will drag it adiabatically to $x_{\rm f}$ in the time interval $[0, 2t^*]$.

We obtain a steadily moving external potential by modulating OL in Eq. (19), thus the MW solitons can manipulate from one stable fixed point to an arbitrary position. Figure 4 demonstrates how to use an OL as a means of an MW soliton at will. Figure 4(a) shows that a moving external potential transfers from a fixed point (here, $x_{\rm i} = -26.17$) to the desired location ($x_{\rm f} = 25.00$) presented in left panel. The manipulation of the MW soliton by modulating a periodic OL, similar to the transferring, drags the condensate along a channel, in which a certain path is installed. The right panel shows the potentials at $t = 0$ and $t = 2t^*$. More specifically, it is an image of potentials in which the condensate is placed at the initial position and the final location, respectively. In this panel, the MW soliton is deposited at point A (a fixed point $x_{\rm i} = -26.17$), then manipulated successfully to the final position point B. Notice that the strength of external potential almost does not change in the whole dragging, it only has a translation. The MW soliton

evolution dynamics in this case is demonstrated in Fig. 4(b): the condensate is trapped at a fixed point ($x_{\rm i} = -26.17$) where it is initially captured, and then

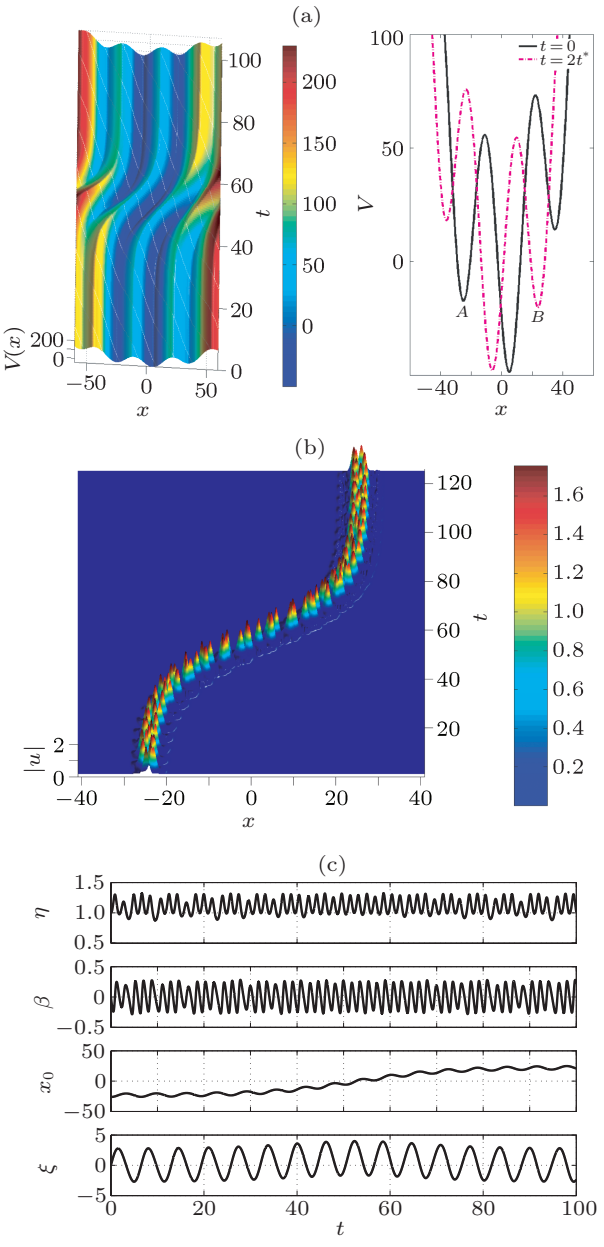


Fig. 4. (colour online) Controllable manipulation of an MW soliton by modulating the OL in the presence of a parabolic potential. (a) The left panel shows space-time plots of the external potential for Eq. (19). The right panel shows potentials of the MW soliton at $t = 0$ and $t = 2t^*$, respectively. (b) Successful dragging by direct numerical simulation of the bright soliton corresponding to that in panel (a) with $V_0 = -50.0$. The parameter values are $A = 1.5$, $V_1 = 0.05$, $k = 0.1$, $\tau = 20$, $\epsilon = 0.001$, $x_{\rm i} = -26.17$, and $x_{\rm f} = 25.00$. The initial conditions are $(\eta,\ \beta,\ x_0, \xi) = (1, 0, -26.17, 0)$. (c) The successful manipulation of normalized amplitude (η), chirp (β), central position (x_0), and central frequency (ξ) fluctuation each as a function of time for EVA Eqs. (5)–(8).

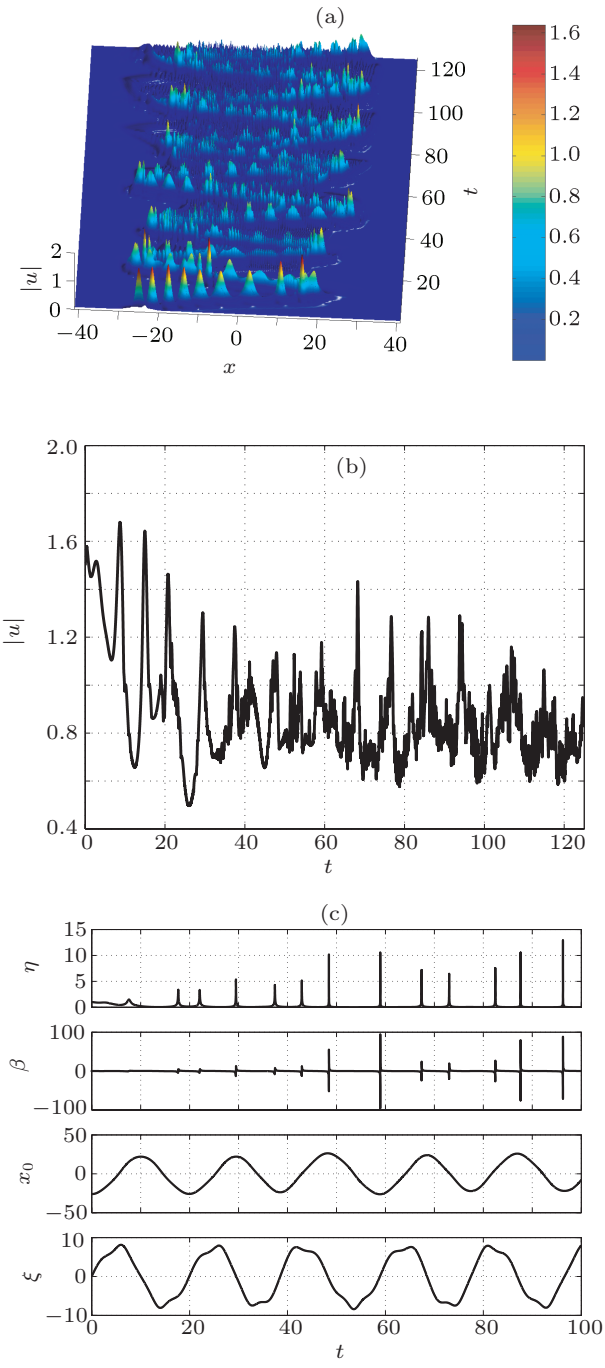


Fig. 5. (colour online) Unsuccessful manipulation of the bright soliton by modulating OL in the presence of a parabolic potential. (a) Failed dragging by direct numerical simulation of the bright soliton corresponding to that in Fig. 4 with the same parameters, but for $V_0 = -10.0$. (b) The time evolution of amplitude $|u|$ of the MW soliton corresponding to that in panel (a). (c) The unsuccessful manipulation of normalized amplitude (η), chirp (β), central position (x_0), and central frequency (ξ) fluctuation each as a function of time for EVA Eqs. (5)–(8).

dragged by the moving OL. In the dragging process, the soliton performs small-amplitude oscillations due to the fact that the fixed point (initial position) is not the most stable lattice site. From Figs. 4(b) and 4(c),

we can draw a conclusion that the manipulation of the variational dynamics is found to be in good agreement with that of the numerical simulations. The flow of the solution in the reduced variables clearly shows the manipulation of the solution from one fixed point to the destination. In addition, we observe the bright MW soliton which can stably evolve and keep conversation of energy, which means that a condensate loaded with information will transmit un-distortedly over a long time in the BEC system.

However, assuming that the parameters are the same with the successful manipulation, but $V_0 = -10$, the MW soliton has dragged unsuccessfully from the fixed point to our desired location. Figure 5 shows the failed dragging of the condensate in the controlled manipulation. In addition, Fig. 5(b) shows that the time dependence of the peak value of wave field $|u|$ drops off to a small value immediately. It is observed that the soliton has collapsed in the evolution of manipulation. Indeed, increasing V_0 to a critical value, the dragging of the condensate may fail.

Our next objective is to find a stable region to determine the relation between adiabaticity and various parameters, such as the strength of the OL V_0 or different strengths of parabolic potential V_1, and adiabaticity parameter τ. In order to successfully drag a condensate outward to our target location from the fixed point, we have found a stable region to manipulate the soliton. As shown in Fig. 6, the various curves in the figure represent the parameter boundaries for the successful dragging of the bright soliton for different parabolic trap strengths (strength increasing from top to bottom). All the curves for different strengths are qualitatively similar, corresponding to higher values of the adiabaticity parameter as the strength is reduced. However, we may fail to drag the condensate with the small adibaticity parameter.

A general trend observed with the increase of the strength of OL V_0 results in failure to drag the MW solitons. At intermediate values of V_0, above which bright MW solitons suffer from failing to manipulate (the area above each curve). For the several lines, when V_0 increases above a critical value V_0, the manipulation of the soliton is almost destroyed (in this case, the evolution leads to the emergence of a collapse state).

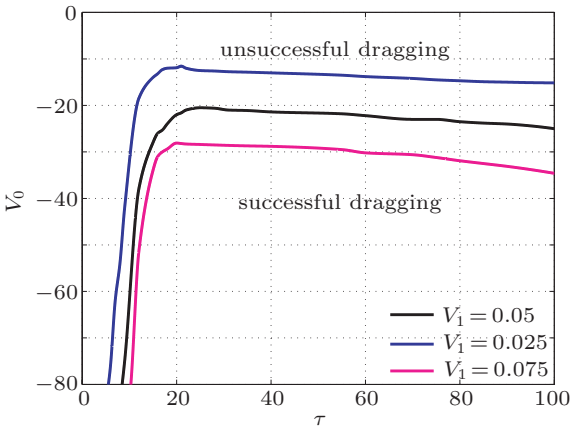


Fig. 6. (colour online) Parameter regions for successful manipulation of MW solitons in the presence of a parabolic and an OL potential. The area below each curve corresponds to the successful dragging region.

5. Conclusion

How to manage and manipulate the condensate has now become a central issue in the study of BEC matter waves. In this work, we introduce an EVA for characterizing the dynamics of the MW solitons subject to a parabolic magnetic potential and a time-space periodic optical lattice. Moreover, simple analytic results also provide a threshold value on the relative strength of the parabolic trap and the OL to obtain multiple stable lattice sites by means of EVA. We then use the OL as a tool to manipulate the solitons. In particular, we find a stable region in which the condensate can be successfully dragged from a fixed point to our destination. Such additional studies may provide a more comprehensive understanding of physics of manipulating MW solitons. There will be a great prospect to guide the manipulation of MW solitons for quantum information and signal processing in experiment. The analysis reported in this paper can be extended to the study of the dynamics, similar dragging and manipulation of high-dimensional solitons. The specific related work is currently in progress.

References

[1] Anderson M H, Matthews J R and Wieman C E 1995 *Science* **269** 198
[2] Dalfovo F, Giorgini S, Pitaevskii L P and Stringari S 1999 *Rev. Mod. Phys.* **71** 463
[3] Anderson B P and Kasevich M A 1998 *Science* **282** 1686
[4] Ovchinnikov Y B, Muller J H, Doery M R, Vredenbregt E J, Helmerson K, Rolston S L and Phillips W D 1999 *Phys. Rev. Lett.* **83** 284
[5] Jaksch D, Bruder C, Cirac J I, Gardiner C W and Zoller P 1998 *Phys. Rev. Lett.* **81** 3108

[6] Choi D I and Niu Q 1999 *Phys. Rev. Lett.* **82** 2022

[7] Carr L D and Brand J 2004 *Phys. Rev.* A **70** 033607

[8] Cornish S L, Claussen N R, Roberts J L, Cornell E A and Wieman C E 2000 *Phys. Rev. Lett.* **85** 1795

[9] Qian C, Wang L L and Zhang J F 2011 *Acta Phys. Sin.* **60** 064214 (in Chinese)

[10] Burlak G and Malomed B A 2008 *Phys. Rev.* A **77** 053606

[11] Brazhnyi V A and Konotop V V 2005 *Phys. Rev.* A **72** 033615

[12] Kevrekidis P G, Theocharis G, Frantzeskakis D J and Malomed B A 2003 *Phys. Rev. Lett.* **90** 230401

[13] Jona-Lasinio M, Morsch O, Cristiani M, Malossi N, Müller J H, Courtade E, Anderlini M and Arimondo E 2003 *Phys. Rev. Lett.* **91** 230406

[14] Caul C, Lima R P A, Diaz E, Müller C A and Domínguez-Adame F 2009 *Phys. Rev. Lett.* **102** 255303

[15] Greiner M, Mandel O, Esslinger T, Hflnsch T W and Bloch I 2002 *Nature* (London) **415** 39

[16] Herring G, Kevrekidis P G, Carretero-González R, Malomed B A, Frantzeskakis D J and Bishop A R 2005 *Phys. Lett.* A **345** 144

[17] Carretero-González R, Frantzeskakis D J and Kevrekidis P G 2008 *Nonlinearity* **21** R139

[18] Strecker K E, Partridge G B, Truscott A G and Hulet R G 2002 *Nature* (London) **417** 150

[19] Pitaevskii L P 1961 *Sov. Phys. JETP* **13** 451

[20] Pérez-García V M, Michinel H and Herrero H 1998 *Phys. Rev.* A **57** 3837

[21] Morsch O and Oberthaler M 2006 *Rev. Mod. Phys.* **78** 179

[22] Brazhnyi V A and Konotop V V 2004 *Mod. Phys. Lett.* B **18** 627

[23] Khaykovich L, Schreck F, Ferrari G, Bourdel T, Cubizolles J, Carr L D, Castin Y and Salomon C 2002 *Science* **296** 1290

[24] Ablowitz M and Segur H 1981 *Solitons and the Inverse Scattering Transforms* (Philadelphia: SIAM)

[25] Elgin J N 1993 *Phys. Rev.* A **47** 4331

[26] Whitham G 1974 *Linear and Nonlinear Waves* (New York: Wiley-Interscience)

[27] Desaix M, Anderson D and Lisak M 1991 *J. Opt. Soc. Am.* B **8** 2082

[28] Pérez-García V M, Michinel H, Cirac J I, Lewenstein M and Zoller P 1997 *Phys. Rev.* A **56** 1424

[29] Anderson D 1983 *Phys. Rev.* A **27** 3135

[30] Malomed B A 2002 *Prog. Opt.* **43** 69

[31] Brand J and Kolovsky A R 2006 *Eur. Phys. J.* D **10** 1140

[32] Trombettoni A and Smerzi A 2001 *Phys. Rev. Lett.* **86** 2353

[33] Drazin P G 1992 *Nonlinear Systems* (Cambridge: Cambridge University)

[34] Zong F D, Yang Y and Zhang J F 2009 *Acta Phys. Sin.* **58** 3670 (in Chinese)

[35] Matuszewsiki M, Malomed B A and Trippenbach M 2007 *Phys. Rev.* A **75** 063621

[36] Kevrekids P G, Frantzeskakis D J, Carretero-González R, Malomed B A, Herring G and Bishop A R 2005 *Phys. Rev.* A **71** 023614

[37] Nistazakis H E, Kevrekidis P G, Malomed B A, Frantzeskakis D J and Bishop A R 2002 *Phys. Rev.* E **66** 015601

[38] Theocharis G, Frantzeskakis D J, Carretero-González R, Kevrekidis P G and Malomed B A 2005 *Phys. Rev.* E **71** 017602